PMUT-Powered Photoacoustic Detection
Revolutionizing Microfluidic Concentration Measurements

Roy, Kaustav; Kumar, Akshay; Shastri, Vijayendra; Munjal, Isha; Kalyan, Kritank; Ashok, Anuj; Jeyaseelan, Antony; Prakash, Jaya; Pratap, Rudra

DOI
10.1109/TIM.2024.3398109

Publication date
2024

Document Version
Final published version

Published in
IEEE Transactions on Instrumentation and Measurement

PMUT-Powered Photoacoustic Detection: Revolutionizing Microfluidic Concentration Measurements

Kaustav Roy, Akshay Kumar, Vijayendra Shastri, Isha Munjal, Kritank Kalyan, Anuj Ashok, Antony Jeyaseelan, Jaya Prakash, *Member, IEEE*, and Rudra Pratap, *Senior Member, IEEE*

***Abstract*— This report introduces a novel optofluidic platform based on piezo-microelectromechanical systems (MEMS) technology, capable of identifying subtle variations in the fluid concentration. The system utilizes piezoelectric micromachined ultrasound transducers (PMUTs) as receivers to capture sound waves produced by nanosecond photoacoustic (PA) pulses emanating from a fluid target housed in PDMS microchannels. Additionally, a dedicated low-noise single-channel amplifier has been developed to extract the minute analog voltage signals from the PMUTs, given the inherently weak ultrasound signals generated by fluid targets. The PMUTs' proficiency in detecting changes in fluid concentration under both static and time-varying conditions has been documented and verified, confirming the platform's efficacy in monitoring fluid concentrations.**

***Index Terms*— Microelectromechanical systems (MEMS), microfluidics, photoacoustics, piezoelectric micromachined ultrasound transducer (PMUT), ultrasound.**

I. Introduction

LIQUIDS are crucial across many industries such as pharmaceuticals, oil and gas, petrochemicals, automotive, and processing sectors. The dye industry, which is vital for producing colors for food, textiles, photography, and leather, depends on solvents to manage dye concentrations. Over time, the concentration of colorants in dye-solvent mixtures decreases [1], making it essential to monitor these concentrations. Despite its importance, there are limited studies on this topic [2].

The transducer field has undergone significant evolution, notably with the introduction of nanotechnology [3], [4], [5], [6], enabling the creation of ultrasmall transducers with submicrometer sizes. This advancement, alongside progress in materials science, led to the development of microelectromechanical systems (MEMS) [7], [8], [9]. This shift to microscale sensors increased their demand, with MEMS inertial systems now commonly found in most smartphones [10]. This shift to microscale sensors increased their demand, with MEMS inertial systems now commonly found in most smartphones. Moreover, MEMS technology has revolutionized ultrasound technology [11], [12] by introducing very small ultrasound transducers, known as micromachined ultrasound transducers (MUTs), which include capacitive MUTs (CMUTs) [13], [14] and piezoelectric MUTs (PMUTs) [15], [15], [16], [17], [18], [19], [20], [21]. Additionally, nanotechnology has played a crucial role in developing miniature fluidic devices such as microvalves [22], micropumps [23], microfluidic flow sensors [24], microneedles [25], and micronozzles [26], among others.

The fusion of light technology with microfluidic systems has led to the emergence of optofluidics [27], a field that combines the advantages of fluidics (such as controlled mixing, stable fluid interfaces, and efficient transport) with the precision of optics (including precise sensing, sub-micrometer light focusing, and object manipulation). This combination has resulted in innovative devices such as fluid lenses [28], optofluidic microscopes [29], and resonators [30]. Moreover, introducing pulsed or modulated light sources into microfluidic systems has advanced the field by using light to induce sound in fluids [31], a process known as photoacoustics. This technique, which generates sound through the exposure of objects to pulsating light, has wide-ranging applications [32], [33], [34], [35], [36]. The combination of light's electromagnetic characteristics and sound's penetration capacity allows for deeper exploration and gathering of valuable data from the targeted subjects.

Recently, there has been a significant increase in the development of PMUT-based photoacoustic devices, especially for deep tissue imaging [37], [38], [39], [40], [41], [42], [43]. PMUTs are preferred for their numerous benefits over

Manuscript received 27 December 2023; revised 29 February 2024; accepted 30 March 2024. Date of publication 23 May 2024; date of current version 31 May 2024. This work was supported by the Department of Science and Technology (DST NanoMission), the Ministry of Education (MOE), the Ministry of Electronics, Information Technology (MeitY) and DBT-IYDF Award under Grant STARS/APR2019/NS/653/FS. The Associate Editor coordinating the review process was Dr. Chao Tan. *(Corresponding authors: Jaya Prakash; Rudra Pratap.)*

Kaustav Roy was with the Centre for Nano Science and Engineering, Indian Institute of Science, Bengaluru 560012, India. He is now with the Department of Electrical and Computer Engineering, Cornell University, Ithaca, NY 14850 USA (e-mail: kaustav@alum.iisc.ac.in).

Akshay Kumar, Antony Jeyaseelan, and Rudra Pratap are with the Centre for Nano Science and Engineering, Indian Institute of Science, Bengaluru 560012, India (e-mail: akshaykumar1@iisc.ac.in; antonya@iisc.ac.in; pratap@iisc.ac.in).

Vijayendra Shastri is with the Department of Precision and Microsystems Engineering, TU Delft, 2628 CD Delft, The Netherlands (e-mail: V.U.Shastri@tudelft.nl).

Isha Munjal and Jaya Prakash are with the Department of Instrumentation and Applied Physics, Indian Institute of Science, Bengaluru 560012, India (e-mail: isha17774@iisc.ac.in; jayap@iisc.ac.in).

Kritank Kalyan was with the Singh Center for Nanotechnology, University of Pennsylvania, Philadelphia, PA 19104 USA. He is now with Zepsor Technologies, Burlington, MA 01803 USA (e-mail: kritank@upenn.edu).

Anuj Ashok is with the Elmore Family School of Electrical and Computer Engineering, Purdue University, West Lafayette, IN 47907 USA (e-mail: anujashok@gmail.com).

Digital Object Identifier 10.1109/TIM.2024.3398109

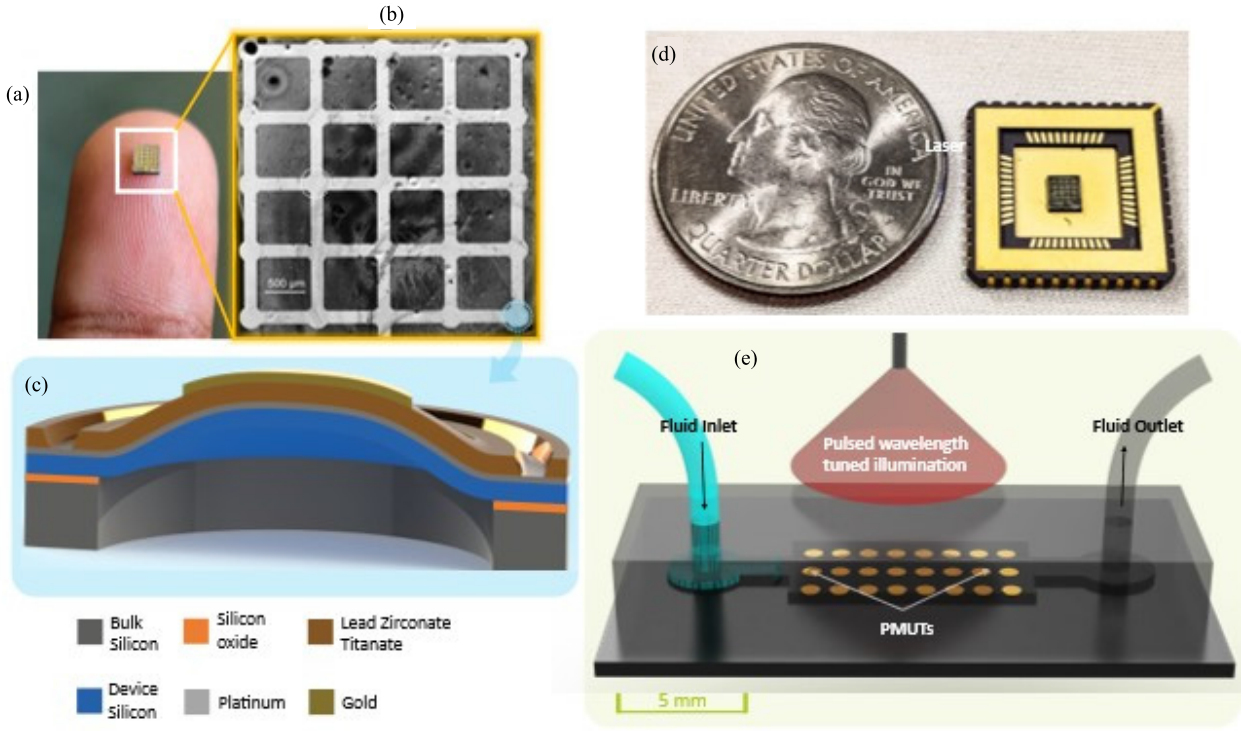

Fig. 1. PMUT-based photoacoustic detection. (a) Picture of the PMUT die used in the work. (b) Zoomed in microscopic view of the PMUT die containing 25 cells connected together to form one single element. (c) Stacked 3-D schematic showing the constitutive layers of a PMUT. (d) PMUT die packaged in a chip carrier. (e) Concept futuristic schematic of PMUT integrated microfluidic device with an external tunable pulsed light source as a photoacoustic spectrophotometer (dimension included).

traditional piezoelectric transducers, including their small and scalable size, low power needs, uniformity across devices, compatibility with CMOS processes, and the ability to be mass-produced. They are crafted using precise nanofabrication techniques, offering superior accuracy in creating small-scale designs compared to conventional bulk ceramic ultrasound transducers.

A few studies have explored using PMUTs for sensing concentrations, like detecting sugar levels in solutions [44], using an ultrasound-only method, unlike the photoacoustic approach discussed here.

The advantage of using light in photoacoustics is that it electromagnetically probes the fluid, providing more nuanced information about concentration levels, thus enhancing detection effectiveness.

In this study, we developed functional thin-film piezoelectric material such as lead zirconate titanate, using nanofabrication techniques to create PMUTs for use as photoacoustic receivers. We also fabricated microfluidic channels from PDMS-glass to hold fluid samples. Our experimental setup included a pulsed laser, a microfluidic channel, and PMUTs to test their effectiveness in capturing photoacoustic signals. We developed a custom low-noise amplification circuit to help retrieve weak photoacoustic signals from the PMUT receiver. Upon evaluation, PMUTs proved to be viable for photoacoustic endeavors. We proceeded with experiments using various concentrations of commercially available blue ink mixed with deionized (DI) water to serve as fluid photoacoustic targets, confirming the PMUT's ability to discern concentration changes as the ink levels in the DI water were altered. We then extended our effort to build a time dynamic concentration monitoring system which could demonstrate the real-time mixing dynamics, thereby demonstrating the successful application of PMUT-powered photoacoustics as detectors of species concentration.

II. PMUT and Microfluidic Channels Used in the Work

A. PMUTs

Piezoelectric MUTs (PMUTs) are advanced acoustic devices made using thin-film piezoelectric materials through micro/nanofabrication techniques. They consist of layered microplates or micromembranes, including bulk silicon, silicon dioxide, device silicon, platinum, lead zirconate titanate (PZT), and gold. The PZT layer, in particular, is crucial for the PMUT's function, enabling it to act as both a transmitter and receiver of acoustic signals. Fig. 1(a) depicts the PMUT die used in this work and Fig. 1(b) depicts a zoomed-in microscopic picture of the die showing a connected matrix of 25 PMUT cells that work together to form the receiver element. The PMUT consists of six different thin-film layers as depicted in Fig. 1(c), such as the bulk silicon, silicon-di-oxide, device silicon, platinum, lead zirconate titanate, and gold. The bulk silicon serves as the handle layer, whereas the device silicon serves as the structural layer, thereby giving the PMUT most of their structural properties. The thin film of PZT acts as the active layer which either vibrates the diaphragm or gets charged upon diaphragm movement. Consequently, a PMUT can function as a transmitter, receiver, or both. The PZT thin

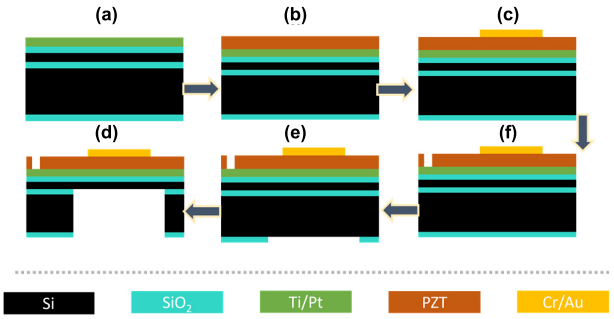

Fig. 2. Fabrication process flow for a PZT-based thin-film PMUT.

film was deposited onto a silicon-on-insulator (SOI) substrate with a uniform device layer thickness of 10 μm. A PMUTs' properties can be customized by adjusting the device layer's dimensions, modifying the combined layer thickness, and altering the fabrication stresses between layers. Postfabrication, the PMUT was connected to a ceramic package with a pin grid array and covered with parylene-c to improve resistance to noise, as illustrated in Fig. 1(d). A futuristic representation of the microfluidic integrated micro photoacoustic device having an array of PMUTs integrated as receivers is depicted in Fig. 1(e). With a wavelength tunable light source, such a device can be used as an ON-chip spectrophotometer to detect and analyze fluid samples.

B. PMUT Fabrication

The PMUTs used in this study were produced following the procedure depicted in Fig. 2. This method begins with a SOI wafer coated with titanium/platinum and featuring a 10 μm thick device layer [Fig. 2(a)]. Through multiple repetitions of the sol–gel method, lead zirconate titanate (PZT) is spin-coated to attain the required thickness (approximately 0.5 μm), followed by an annealing process at 650 °C to create a consistent thin film [Fig. 2(b)]. Next, the upper electrode (Chrome/Gold — 30/120 nm) is patterned using lithography [Fig. 2(c)], and the PZT layer is subsequently removed through wet etching [Fig. 2(d)]. The composite is then patterned from the rear to eliminate the backside oxide using reactive ion etching (RIE), as illustrated in Fig. 2(e). In the final steps, the supporting layer is etched via deep RIE (DRIE) to release the devices, and the buried oxide is etched away to relieve any residual stress in the released stack Fig. 2(f).

C. PMUT Characterization

PMUT's stack was first optically characterized using the scanning electron microscope (SEM), which revealed the thickness of the deposited thin-film PZT to be 1.25 μm, without any inherent observable defects [Fig. 3(a)]. Postpiezoelectric poling, one of the typical cells in the PMUT die is characterized materially, to understand the properties of the piezoelectric thin film, electrically, to determine the electrical impedance of the device and mechanically, to determine the device deflection sensitivity. The electrical quality of the PZT thin film was evaluated through polarization, achieved by varying the voltage using a Precision Materials Analyzer (Radiant

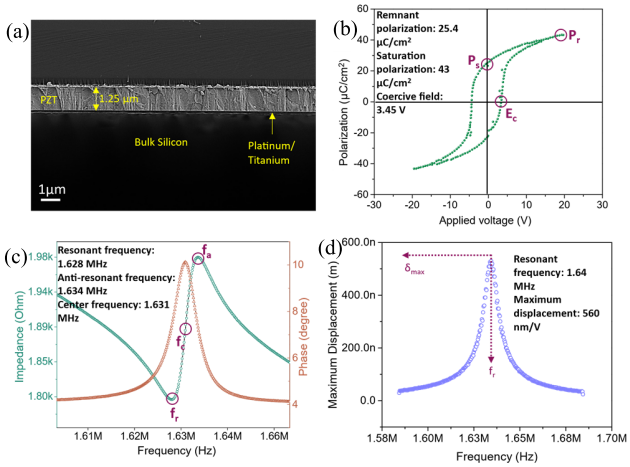

Fig. 3. PMUT characterization. (a) Optical: SEM of PMUT's stack. (b) Material: polarization versus voltage hysteresis loop. (c) Electrical: absolute electrical impedance and phase versus frequency. (d) Mechanical: maximum displacement of the PMUT versus frequency.

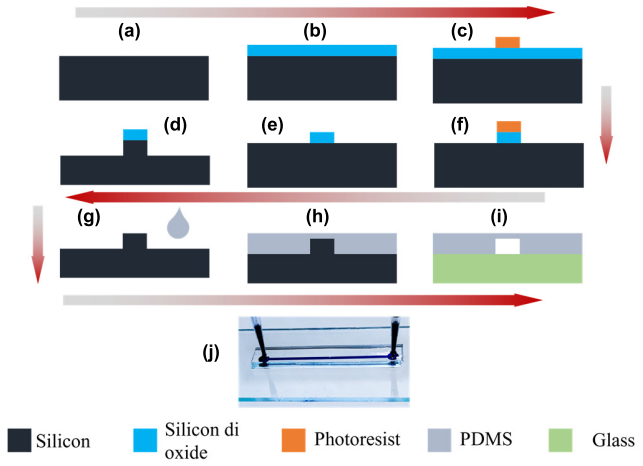

Fig. 4. Process flow for making the microfluidic channel on glass.

Technologies Inc.). The resulting hysteresis loop is depicted in Fig. 3(b), displaying the characteristic ferroelectric switching of the PZT thin film in response to the applied electric field. Key parameters extracted from the graph include the remanent polarization (P_r), saturated polarization (P_s), and the coercive field (E_c), measured at 25.4 μC/cm^2, 43 μC/cm^2, and 3.45 V, respectively. To understand the ac characteristics of the device, electrical characterization was conducted using 4294A Precision Impedance Analyzer, Agilent Inc., and the results obtained are shown in Fig. 3(c). The frequency was swept from 1.61 to 1.66 MHz. The maximum impedance magnitude was found to be 1.98 kΩ, and the minimum impedance magnitude was found to be 1.80 kΩ, respectively. The resonant frequency (f_r), center frequency (f_c), and the antiresonant frequency (f_a) was found to be 1.628, 1.631, and 1.634 MHz, respectively. The effective electromechanical coupling coefficient has been determined to be 0.73%. From the phase spectra, a change of 6° has been observed at resonance. To understand the behavior of the PMUTs mechanically, one of the typical PMUTs was selected from the die and was characterized

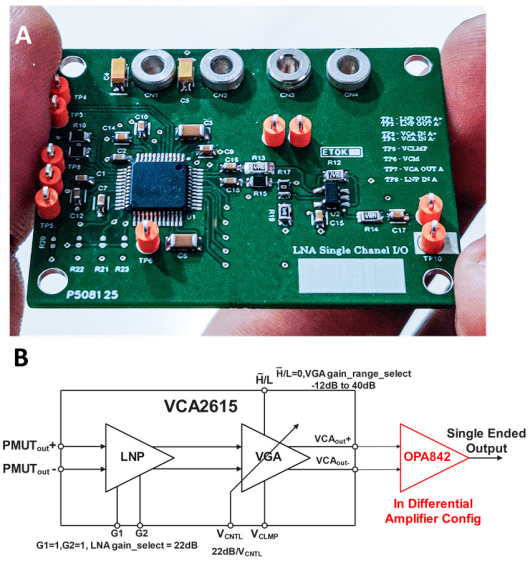

Fig. 5. PMUT signal amplification circuit. (a) Printed circuit board containing the VCA 2615 IC from the Texas Instruments, along with the additional support circuitry. (b) Block diagram of the circuit showing connections in detail.

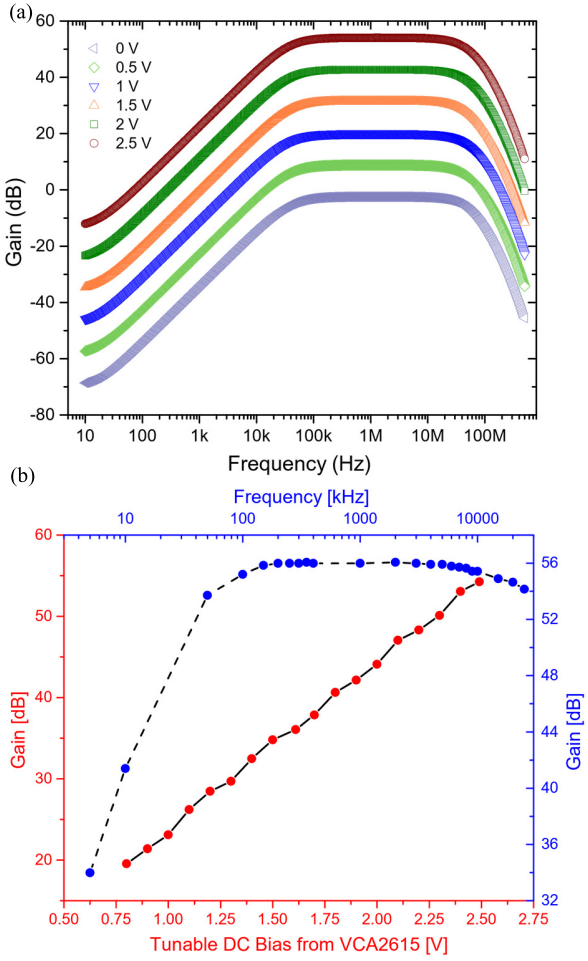

Fig. 6. PMUT amplifier in simulation and characterization. (a) LT SPICE simulation of the designed circuit with a broad gain band from 100 kHz to 10 MHz. (b) Experimental validation by characterizing the amplifier PCB.

using the laser Doppler vibrometer (Microsystems Analyzer, MSA 500) from Polytec Inc. [Fig. 3(d)]. The PMUT cell

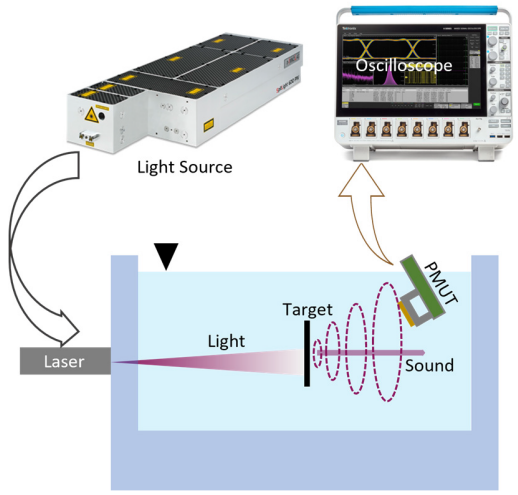

Fig. 7. Schematic of PMUT-PA experimental setup.

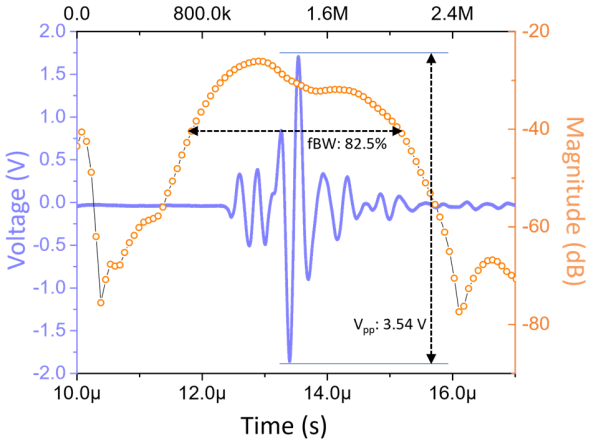

Fig. 8. PA A-line time and frequency domain signal as obtained from the PMUT. The –6 dB fractional bandwidth was observed to be 82.5%. characterizing the PCB.

demonstrated a maximum peak hold deflection of 560 nm/V at a frequency of 1.64 MHz.

D. Fabrication of Microfluidic Devices

The microfluidic channel was developed at NNFC, CeNSE using a series of steps outlined below. Initially, a silicon mold underwent RCA cleaning [Fig. 4(a)], followed by the addition of silicon dioxide to act as a robust mask for later etching phases [Fig. 4(b)]. The substrate that resulted was then coated with a thick layer of AZ4562 photoresist [Fig. 4(c)], after which oxide etching was performed in areas without patterning [Fig. 4(d)] using RIE. Subsequently, the photoresist was removed through ashing [Fig. 4(e)]. The substrate then underwent a timed deep RIE process to achieve a specific depth [Fig. 4(f)], creating the microfluidic mold. Afterward, PDMS, combined with a curing agent in a 10:1 ratio, was poured over the mold [Fig. 4(g)] and set at 120 °C for 30 min. The solidified PDMS was gently peeled off the mold [Fig. 4(h)] and adhered to a glass slide with a plasma etcher from Harrick Plasma Inc. [Fig. 4(i)]. The assembled microfluidic apparatus

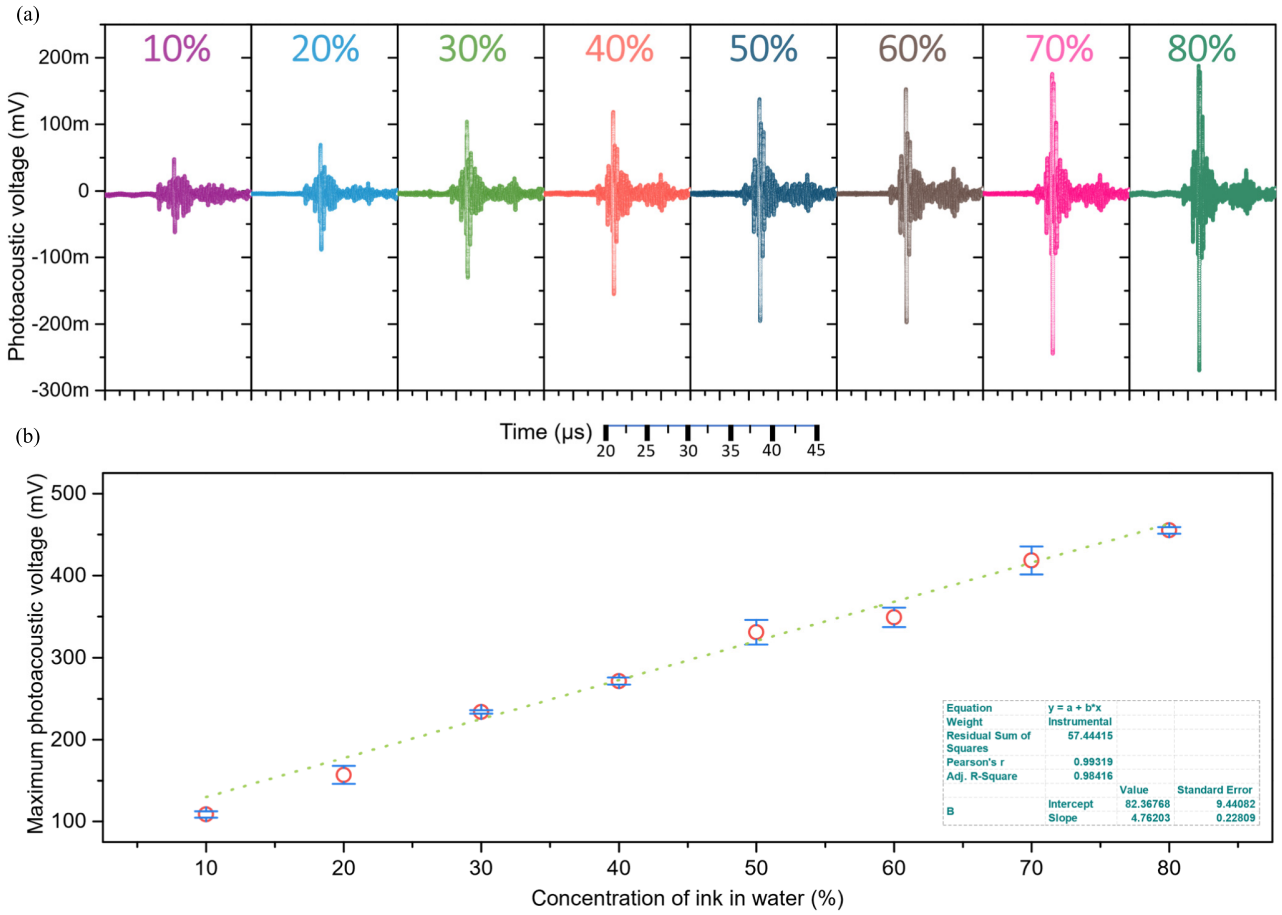

Fig. 9. Static concentration measurements. (a) PA A-line voltage signals as received from the PMUT for ink-water fluid targets confined in microfluidic channels. (b) Maximum PA signal amplitude plotted with ink concentration.

was then heated at 120 °C to reinforce the bond. Fig. 4(j) shows the standard bonded microfluidic device used in the experiment, featuring cross-sectional dimensions of 1000 μm in width and 50 μm in depth.

III. PMUT Photoacoustic Instrumentation

A. PMUT Signal Amplification

In-house, low-noise amplifier (LNA) circuit was designed for low-noise PMUT photoacoustic (PA) signal amplification as shown Fig. 5(a). Fig. 5(b) shows the circuit block diagram. The heart of this circuit consists of a Texas Instrument's VCA2615 IC [45] for excellent input signal handling capabilities, combining low-noise preamplifier (LNP) and a voltage-gain amplifier (VGA) inside the IC. The differential output of VCA 2615 is buffered using a separate OPA842 op-amp in differential amplifier configuration for single-ended output. A +/−5 V power supply is used for the LNA circuit and a dc bench top power supply is used to control the Vcntl, which ultimately controls the VGA gain with the linear control response of 22 dB/V. G1 and G2 are held high for 22 dB LNP gain settings as at this setting achieves 0.7 nV/$\sqrt{\text{Hz}}$ voltage noise and typically 1 pA/$\sqrt{\text{Hz}}$ current noise. H/L pin is held low for +6 dB discrete gain. For limiting the amplified output voltage swing, V_{clmp} can be used as input voltage reference for output clipping to desired voltage level. Fig. 6 shows the characterization of the constructed amplifier circuit by simulation [see Fig. 6(a)] and by actual experiment [see Fig. 6(b)]. The simulation and the experiment tests closely match with a broad gain band from 100 kHz to 10 MHz of frequencies. The linearity on changing the magnitude of the Vcntl is also observed in both the simulation and the experiment with the gain rising from ∼20 dB at ∼0.75 V to ∼55 dB at 2.5 V.

B. Photoacoustic Setup

Fig. 7 illustrates a diagram outlining the setup for the photoacoustic experiment. This system includes a versatile OPO nanosecond pulsed laser (specifically, the SpitLight 1000 from InnoLas Lasers GmbH), adjustable within the 660–2500 nm wavelength range. This laser has a 7 ns pulsewidth and operates at a repetition rate of 30 Hz. The laser targets a photoacoustic target (microfluidic sample or pencil lead) affixed to the side of a specially designed glass tank, using a 660 nm wavelength. Upon absorbing the fluctuating light, the target generates acoustic signals, which the PMUT detects. The PMUT's voltage output is first amplified by a low-noise, voltage-controlled amplifier (VCA 2615, Texas Inc.), built in-house, before being transmitted to an oscilloscope (Mixed Signal Oscilloscope, Tektronix Inc.). This signal is then relayed to

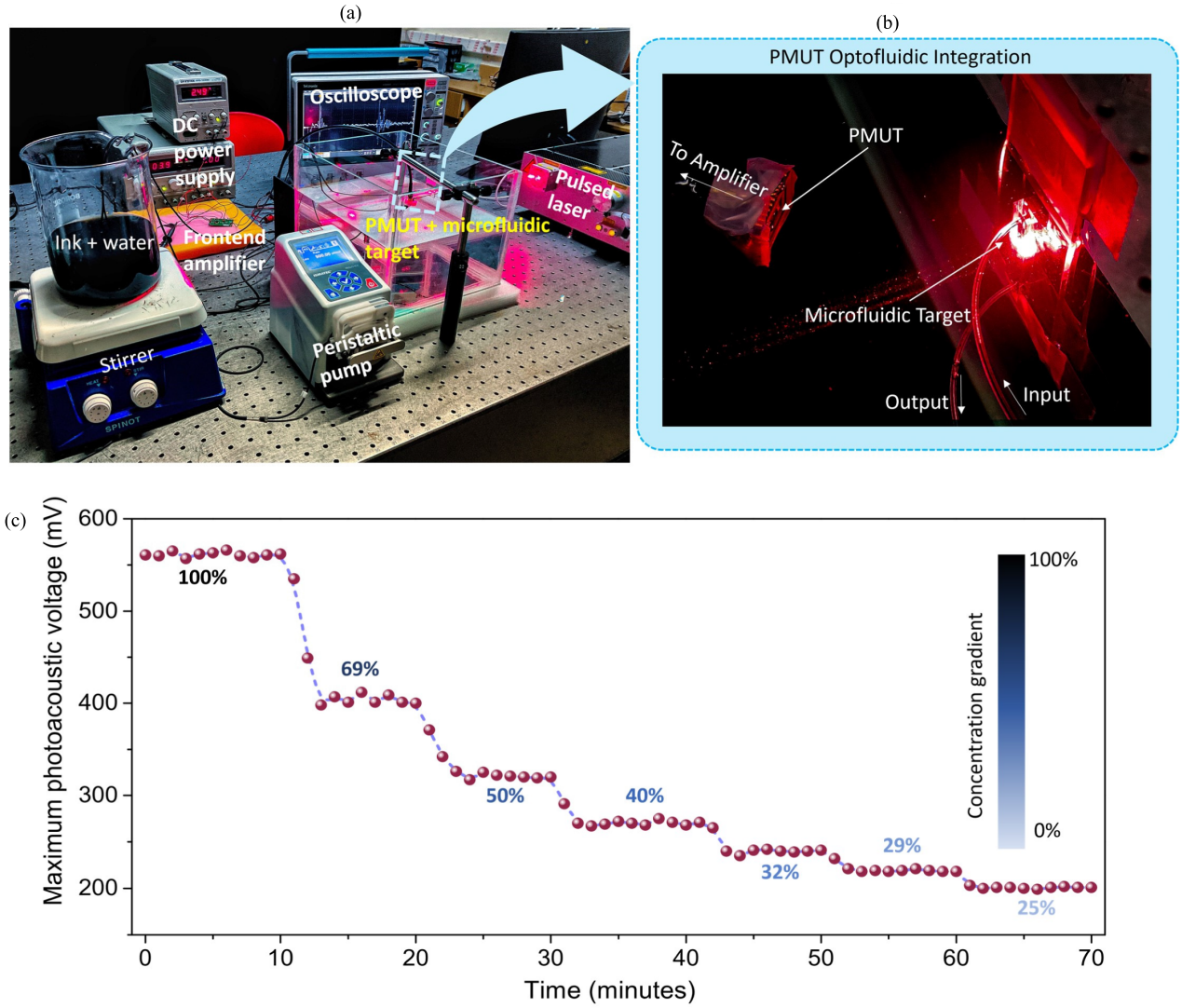

Fig. 10. Real-time concentration measurement. (a) Experimental setup for conducting the real-time concentration monitoring. (b) Zoomed-in view of the PMUT PA microfluidic system. (c) Concentration time dynamics as observed using the PMUT, captured from the fluid inside the microfluidic channel.

a computer for immediate, digitally conditioned visualization. Precise positional adjustments of the PMUT are made possible through an x–y linear stage (CONEX-TRA25CC, Newport Inc.), with movements directed by specialized software on the computer. Additionally, the computer governs the pulsed laser, producing precise triggers that are in sync with the oscilloscope, thereby facilitating exact dynamic assessments.

IV. Results

A. PA A-Line

In this study, the packaged PMUT was evaluated as an acoustic sensor using the previously described experimental arrangement. A pencil lead with a circular cross section and a diameter of 500 μm served as the target for photoacoustic emissions during laser exposure to pulsed nanosecond light, positioned 5 cm from the PMUT's surface. The collected data are presented in Fig. 8. The PMUT registered a peak-to-peak voltage of 3.54 V on the oscilloscope after amplification by 55 dB, equating to an original signal of 6.29 mV from the PMUT. An A-line data analysis was conducted using a fast Fourier transform (FFT), with the results depicted in Fig. 8. The predominant frequency in water was identified as 1.12 MHz. Additionally, the fractional −6 dB bandwidth was computed, revealing a value of 82.5%.

B. Static Concentration Measurements

The PMUT PA microfluidic concentration detector was next used to detect the change in concentration for particular fluid mixtures. India ink along with DI water was used as the light absorbing target solution, which was injected into the microfluidic target, adhered to one of the walls of the transparent container (Fig. 7). The packaged PMUT die was kept at an angle as depicted in Fig. 7, for the reception of the photoacoustic signal generated from the microfluidic target. Both the microfluidic target and the packaged PMUT were submerged under water for efficient acoustic coupling. Eight different concentrations were prepared from 10% (10 mL in 90 mL of DI water) to 80% (80 in 20 mL of DI water) in steps of 10%. The time domain PA A-line obtained from

each target concentrations are depicted in Fig. 9(a). All of the A-line signals follow the same observable pattern. The peak-to-peak voltage magnitude was extracted from the A-lines obtained from each different concentration and plotted as depicted in Fig. 9(b). A linear fit with a r-squared of 0.99 was obtained suggesting a linear relationship between the peak-to-peak voltage magnitude and the species concentration. The slope of the fit line suggests a sensitivity of 4.8 mV/% change in concentration.

C. Real-Time Concentration Measurements

Next, in order to establish the PMUT PA-microfluidic platform as a real-time concentration detector, the setup was enhanced by the addition of a mixture reservoir with an associated stirrer and a peristaltic pump Reglo ICC from Ismatec Inc. to circulate the reservoir fluid real time through the microfluidic channel, at a flow rate of 60 mL/min while illuminating the channel constantly with the pulsed light in the wavelength of 660 nm. Fig. 10(a) depicts the experimental setup used for the real-time concentration measurements showing the necessary parts. Fig. 10(b) represents the zoomed-in view of the PMUT optofluidic integration showing the PMUT, light, and the microfluidic target. The plot obtained from Fig. 10(c) shows the time dynamics of the concentration change as tracked by the PMUT PA microfluidic detector. The experiment was initialized with 200 mL of a blue colored India ink in the reservoir which was circulated through the microfluidic channel for the first 10 min. The maximum PA voltage obtained was noted at ∼550 mV. After 10 min, 100 mL of DI water was added to the reservoir. The voltage was observed to drop for the next 4 min, thereby reaching saturation at ∼400 mV. The concentration of ink to water at this level of mixture was 69%. DI water was continually added after every 10 min till 70 min of time until the real-time voltage to time curve hit saturation. As the experiment progressed, with each new volume addition in water the magnitude of the decrease in voltage was found to be lower as compared to the previous addition, revealing the nonlinear nature of the mixing.

V. Conclusion

We designed and built a multimodal sensor platform by leveraging the confluence of different domains such as photoacoustics, microfluidics, spectrometry, and thin-film piezo-MEMS. We demonstrated the capability of such an interdisciplinary sensor platform to independently detect dye concentration with a sensitivity of 4.8 mV/% change in concentration, having a response time of less than 1 s and a resolution of 0.5%, thereby proving useful for several applications where detection of dissolved species concentration in a fluid plays a pivotal role. Our home-built instrumentation setup employed piezo-MEMS ultrasound transducer (PMUT) to receive sound waves generated by nanosecond PA pulses from a fluid sample contained within PDMS microchannels. A specialized low-noise, single-channel voltage-controlled amplifier with a voltage gain of 56 dB was designed and fabricated to capture the weak analog voltage signals from the PMUTs, addressing the challenge of low-intensity ultrasound signals typically emitted by fluid samples. Upon interfacing the PMUT receiver with the amplifier, we tested the PMUT's bandwidth to photoacoustic nanosecond impulse. A fractional bandwidth of 82.5% was observed in water. As a final capability check, we applied the platform to sense fluid concentration alterations, both in static and dynamic scenarios. The static concentration detection demonstrated linear detection characteristics which directly follows the Beer Lambert absorption law, thereby proposing the use of such a platform for microfluidic spectrometric measurements. The dynamic concentration measurement lasted for 70 min and confirmed the fit of the platform as a continuous fluid health-monitoring unit.

Although our contribution is novel, there can be several developments needed to make an advanced PMUT-based microfluidic spectrometer: 1) heterogeneous integration of CMOS chips to PMUTs to make the receive electronics in a microscopic form factor; 2) having a PMUT-microfluidic-integration with LED/laser diodes integrated in the chip as portable photoacoustic sources; and 3) introducing the laser wavelength tunability to leverage spectral unmixing of a mixture of species, thereby enabling multiplexed detection.

Acknowledgment

The authors are grateful to all the staff at the National Nanofabrication Centre (NNFC), Micro Nano Characterization Facility (MNCF) at the Centre for Nano Science and Engineering (CeNSE), Indian Institute of Science.

References

[1] M. Ueda, S. Mizuno, A. Matsumura, and F. Sakan, "Real-time optical monitoring system for dye colour and concentration," *Opt. Lasers Eng.*, vol. 25, no. 1, pp. 13–23, Jul. 1996, doi: 10.1016/0143-8166(95)00082-8.

[2] P. Poscio, Y. Emery, P. Bauerfeind, and C. Depeursinge, "In vivo measurement of dye concentration using an evanescent-wave optical sensor," *Med. Biol. Eng. Comput.*, vol. 32, no. 4, pp. 362–366, Jul. 1994.

[3] D. Li, A. Yadav, H. Zhou, K. Roy, P. Thanasekaran, and C. Lee, "Advances and applications of metal-organic frameworks (MOFs) in emerging technologies: A comprehensive review," *Global Challenges*, vol. 8, no. 2, Feb. 2024, Art. no. 2300244.

[4] V. Shastri, S. Majumder, A. Ashok, K. Roy, R. Pratap, and P. Kumar, "Electric current-assisted manipulation of liquid metals using a stylus at micro- and nano-scales," *Nanotechnology*, vol. 34, no. 10, Mar. 2023, Art. no. 105301.

[5] V. Shastri, S. Talukder, K. Roy, P. Kumar, and R. Pratap, "Manipulating liquid metal flow for creating standalone structures with micro-and nano-scale features in a single step," *Nanotechnology*, vol. 33, no. 45, Nov. 2022, Art. no. 455301.

[6] V. Shastri, S. Talukder, K. Roy, P. Kumar, and R. Pratap, "Spontaneous formation of structures with micro- and nano-scopic periodic ripple patterns," *ACS Omega*, vol. 7, no. 14, pp. 12111–12119, 2022.

[7] R. Bogue, "Recent developments in MEMS sensors: A review of applications, markets and technologies," *Sensor Rev.*, vol. 33, no. 4, pp. 300–304, Sep. 2013.

[8] S. Harsha Paladugu, K. Roy, A. Ashok, B. Nayak, A. Rangarajan, and R. Pratap, "Boosting resonant sensing in fluids: A surprising discovery," 2023, *arXiv:2312.05214*.

[9] R. Pratap, A. Dangi, K. Roy, and H. Gupta, "(Invited) fluid spectroscopy with piezoelectric ultrasound MEMS transducers," *ECS Trans.*, vol. 86, no. 16, pp. 13–20, Jul. 2018, doi: 10.1149/08616.0013ecst.

[10] B. Vigna, "Future of MEMS: An industry point of view," in *Proc. 7th. Int. Conf. Thermal, Mech. Multiphys. Simulation Exp. Micro-Electron. Micro-Syst.*, 2006, pp. 1–8.

[11] K. Roy et al., "Body conformal linear ultrasound array for combined ultrasound and photoacoustic imaging," in *Proc. IEEE Int. Ultrason. Symp. (IUS)*, Sep. 2020, pp. 5–8, doi: 10.1109/ius46767.2020.9251458.

[12] M. Mitra et al., "Low-cost scalable PCB-based 2-D transducer arrays for volumetric photoacoustic imaging," *IEEE Sensors J.*, vol. 24, no. 4, pp. 4380–4386, Feb. 2024.

[13] E. Moisello, L. Novaresi, E. Sarkar, P. Malcovati, T. L. Costa, and E. Bonizzoni, "PMUT and CMUT devices for biomedical applications: A review," *IEEE Access*, vol. 12, pp. 18640–18657, 2024.

[14] J. Joseph, B. Ma, and B. T. Khuri-Yakub, "Applications of capacitive micromachined ultrasonic transducers: A comprehensive review," *IEEE Trans. Ultrason., Ferroelectr., Freq. Control*, vol. 69, no. 2, pp. 456–467, Feb. 2022.

[15] K. Roy, J. E.-Y. Lee, and C. Lee, "Thin-film PMUTs: A review of over 40 years of research," *Microsyst. Nanoeng.*, vol. 9, no. 1, p. 95, Jul. 2023.

[16] K. Roy et al., "Fluid density sensing using piezoelectric micromachined ultrasound transducers," *IEEE Sensors J.*, vol. 20, no. 13, pp. 6802–6809, Jul. 2020.

[17] K. Roy, A. Mandal, A. Ashok, H. Gupta, V. Shastri, and R. Pratap, "A single cell PMUT as a bio-fluid density sensor," in *Proc. IEEE Int. Ultrason. Symp. (IUS)*, Sep. 2020, pp. 1–4, doi: 10.1109/IUS46767.2020.9251809.

[18] H. Gupta, B. Nayak, K. Roy, A. Ashok, A. Jeyaseelan, and R. Pratap, "Development of micromachined piezoelectric near-ultrasound transducers for data-over-sound," in *Proc. IEEE Int. Ultrason. Symp. (IUS)*, Sep. 2020, pp. 1–4, doi: 10.1109/IUS46767.2020.9251747.

[19] B. Nayak, H. Gupta, K. Roy, A. Ashok, V. Shastri, and R. Pratap, "An experimental study of the acoustic field of a single-cell piezoelectric micromachined ultrasound transducer (PMUT)," in *Proc. 5th IEEE Int. Conf. Emerg. Electron. (ICEE)*, Nov. 2020, pp. 1–4, doi: 10.1109/ICEE50728.2020.9777041.

[20] K. Roy, K. Kalyan, A. Ashok, V. Shastri, and R. Pratap, "A pmut integrated microfluidic system for volumetric flow rate sensing," in *Proc. 21st Int. Conf. Solid-State Sensors, Actuators Microsyst. (Transducers)*, Jun. 2021, pp. 172–175, doi: 10.1109/Transducers50396.2021.9495576.

[21] K. Roy et al., "A PMUT integrated microfluidic system for fluid density sensing," *J. Microelectromech. Syst.*, vol. 30, no. 4, pp. 642–649, Aug. 2021, doi: 10.1109/JMEMS.2021.3091651.

[22] J.-Y. Qian, C.-W. Hou, X.-J. Li, and Z.-J. Jin, "Actuation mechanism of microvalves: A review," *Micromachines*, vol. 11, no. 2, p. 172, Feb. 2020.

[23] D. J. Laser and J. G. Santiago, "A review of micropumps," *J. Micromech. Microeng.*, vol. 14, no. 6, pp. R35–R64, Jun. 2004, doi: 10.1088/0960-1317/14/6/r01.

[24] A. Rasmussen, C. Mavriplis, M. E. Zaghloul, O. Mikulchenko, and K. Mayaram, "Simulation and optimization of a microfluidic flow sensor," *Sens. Actuators A, Phys.*, vol. 88, no. 2, pp. 121–132, Feb. 2001, doi: 10.1016/s0924-4247(00)00503-3.

[25] G. Ma and C. Wu, "Microneedle, bio-microneedle and bio-inspired microneedle: A review," *J. Controlled Release*, vol. 251, pp. 11–23, Apr. 2017.

[26] R. Bayt, A. Ayon, K. Breuer, R. Bayt, A. Ayon, and K. Breuer, "A performance evaluation of MEMS-based micronozzles," in *Proc. 33rd Joint Propuls. Conf. Exhib.*, Jul. 1997, p. 3169.

[27] X. Fan and I. M. White, "Optofluidic microsystems for chemical and biological analysis," *Nature Photon.*, vol. 5, no. 10, pp. 591–597, Oct. 2011.

[28] N.-T. Nguyen, "Micro-optofluidic lenses: A review," *Biomicrofluidics*, vol. 4, no. 3, Sep. 2010, doi: 10.1063/1.3460392.

[29] X. Heng et al., "Optofluidic microscopy—A method for implementing a high resolution optical microscope on a chip," *Lab Chip*, vol. 6, no. 10, pp. 1274–1276, 2006.

[30] S. I. Shopova, H. Zhou, X. Fan, and P. Zhang, "Optofluidic ring resonator based dye laser," *Appl. Phys. Lett.*, vol. 90, no. 22, pp. 1–4, May 2007, doi: 10.1063/1.2743884.

[31] N. Rossetto, I. Fortunati, C. Gellini, A. Feis, and C. Ferrante, "An optofluidic light detector based on the photoacoustic effect," *Sens. Actuators B, Chem.*, vol. 233, pp. 71–75, Oct. 2016, doi: 10.1016/j.snb.2016.04.046.

[32] S. Manohar and D. Razansky, "Photoacoustics: A historical review," *Adv. Opt. Photon.*, vol. 8, no. 4, p. 586, 2016.

[33] L. V. Wang, "Prospects of photoacoustic tomography," *Med. Phys.*, vol. 35, no. 12, pp. 5758–5767, Nov. 2008.

[34] K. Roy et al., "An optofluidic dye concentration detector based on the pulsed photoacoustic effect," *Proc. SPIE*, vol. 11637, pp. 89–95, Jun. 2021, doi: 10.1117/12.2582656.

[35] J. Yao and L. V. Wang, "Photoacoustic microscopy," *Laser Photon. Rev.*, vol. 7, no. 5, pp. 758–778, Sep. 2013.

[36] V. Ntziachristos and D. Razansky, "Molecular imaging by means of multispectral optoacoustic tomography (MSOT)," *Chem. Rev.*, vol. 110, no. 5, pp. 2783–2794.

[37] A. Paramanick, K. Roy, D. Samanta, K. S. Aiswarya, R. Pratap, and M. S. Singh, "Image quality enhancement of PMUT-based photoacoustic imaging," *Proc. SPIE*, vol. 12379, pp. 386–391, Nov. 2023.

[38] B. Chen, F. Chu, X. Liu, Y. Li, J. Rong, and H. Jiang, "AlN-based piezoelectric micromachined ultrasonic transducer for photoacoustic imaging," *Appl. Phys. Lett.*, vol. 103, no. 3, p. 31118, Jul. 2013, doi: 10.1063/1.4816085.

[39] Y. Wang, J. Cai, T. Wu, and F. Gao, "Photoacoustic dual-mode microsensor based on PMUT technology," in *Proc. IEEE Int. Symp. Circuits Syst. (ISCAS)*, May 2022, pp. 2836–2840.

[40] A. Dangi et al., "A modular approach to neonatal whole-brain photoacoustic imaging," *Proc. SPIE*, vol. 11240, pp. 317–325, Jun. 2020, doi: 10.1117/12.2546854.

[41] J. Cai et al., "Beyond fundamental resonance mode: High-order multiband ALN PMUT for in vivo photoacoustic imaging," *Microsyst. Nanoeng.*, vol. 8, no. 1, pp. 1–12, 2022.

[42] A. Paramanick et al., "Photoacoustic imaging with single-element, low-frequency thin-film PMUT," *IEEE Sensors Lett.*, vol. 8, no. 3, pp. 1–4, Mar. 2024, doi: 10.1109/LSENS.2024.3358105.

[43] K. Roy et al., "Towards the development of backing layer for piezoelectric micromachined ultrasound transducers," *Proc. SPIE*, vol. 11642, pp. 309–314, 2021, doi: 10.1117/12.2582504.

[44] L. Shi, L. Jia, C. Liu, C. Sun, S. Liu, and G. Wu, "A miniaturized ultrasonic sugar concentration detection system based on piezoelectric micromachined ultrasonic transducers," *IEEE Trans. Instrum. Meas.*, vol. 71, pp. 1–9, 2022.

[45] (2008). *Dual, Low-Noise Variable-Gain Amplifier With Preamp*. [Online]. Available: https://www.ti.com/lit/ds/symlink/vca2615.pdf?ts=1698386975094&ref_url=https%253A%252F%252Fwww.ti.com%252Fproduct%252FVCA2615